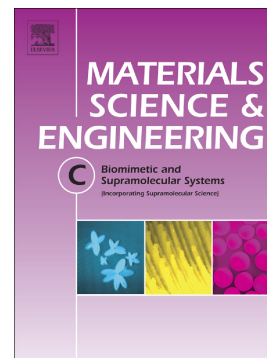


Journal Pre-proof

α -Helical Peptides on Plasma-Treated Polymers Promote Ciliation of Airway Epithelial Cells

Nazia Mehrban, Daniela Cardinale, Santiago C. Gallo, Dani D.H. Lee, D. Arne Scott, Hanshan Dong, James Bowen, Derek N. Woolfson, Martin A. Birchall, Christopher O'. Callaghan



PII: S0928-4931(21)00073-4

DOI: <https://doi.org/10.1016/j.msec.2021.111935>

Reference: MSC 111935

To appear in: *Materials Science & Engineering C*

Received date: 9 November 2020

Revised date: 11 January 2021

Accepted date: 30 January 2021

Please cite this article as: N. Mehrban, D. Cardinale, S.C. Gallo, et al., α -Helical Peptides on Plasma-Treated Polymers Promote Ciliation of Airway Epithelial Cells, *Materials Science & Engineering C* (2021), <https://doi.org/10.1016/j.msec.2021.111935>

This is a PDF file of an article that has undergone enhancements after acceptance, such as the addition of a cover page and metadata, and formatting for readability, but it is not yet the definitive version of record. This version will undergo additional copyediting, typesetting and review before it is published in its final form, but we are providing this version to give early visibility of the article. Please note that, during the production process, errors may be discovered which could affect the content, and all legal disclaimers that apply to the journal pertain.

© 2021 Published by Elsevier.

α -Helical Peptides on Plasma-Treated Polymers Promote Ciliation of Airway Epithelial Cells

Authors

Dr. Nazia Mehrban^{1*}, Dr. Daniela Cardinale², Dr. Santiago C. Gallo³, Dani D.H. Lee², Dr. D. Arne Scott⁴, Prof. Hanshan Dong⁵, Ass. Prof. James Bowen⁶, Prof. Derek N Woolfson^{4,7,8}, Prof. Martin A Birchall¹, Prof. Christopher O'Callaghan²

¹UCL Ear Institute, University College London, 332 Gray's Inn Rd, London, WC1X 8EE, UK, ²Infection, Immunity and Inflammation Department, UCL Great Ormond Street Institute of Child Health, University College London, 30 Guilford St, London, WC1N 1EH, UK, ³Institute for Frontier Materials, Deakin University, 75 Pigdons Rd, Victoria, VIC 3216, Australia, ⁴School of Chemistry, University of Bristol, Cantock's Close, Bristol, BS8 1TS, UK, ⁵School of Metallurgy and Materials, University of Birmingham, Elms Rd, Birmingham, B15 2SE, UK, ⁶School of Engineering & Innovation, The Open University, Walton Hall, Milton Keynes, MK7 6AA, UK, ⁷School of Biochemistry, University of Bristol, University Walk, Bristol, BS8 1TD, UK, ⁸Bristol BioDesign Institute, University of Bristol, 24 Tyndall Avenue, Bristol, BS8 1TQ, UK

**Corresponding author. N. Mehrban (e-mail: n.mehrban@ucl.ac.uk)*

Abstract

Airway respiratory epithelium forms a physical barrier through intercellular tight junctions, which prevents debris from passing through to the internal environment while ciliated epithelial cells expel particulate-trapping mucus up the airway. Polymeric solutions to loss of airway structure and integrity have been unable to fully restore functional epithelium. We hypothesized that plasma treatment of polymers would permit adsorption of α -helical peptides and that this would promote functional differentiation of airway epithelial cells. Five candidate plasma compositions are compared; Air, N₂, H₂, H₂:N₂ and Air:N₂. X-ray photoelectron spectroscopy shows changes in at% N and C 1s peaks after plasma treatment while electron microscopy indicates successful adsorption of hyrogelating self-assembling fibres (hSAF) on all samples. Subsequently, adsorbed hSAFs support human nasal epithelial cell attachment and proliferation and induce differentiation at an air-liquid interface. Transepithelial measurements show that the cells form tight junctions and produce cilia beating at the normal expected frequency of 10-11 Hz after 28 days in culture. The synthetic peptide system described in this study offers potential superiority as an epithelial regeneration substrate over present “gold-standard” materials, such as collagen, as they are controllable and can be chemically functionalised to support a variety of *in vivo* environments. Using the hSAF peptides described here in combination with plasma-treated polymeric surfaces could offer a way of improving the functionality and integration of implantable polymers for aerodigestive tract reconstruction and regeneration.

Keywords: Polymer, Peptide, Plasma Treatment, Cilia, Biomaterial, Airway

1.0 Introduction

The airway is lined with a multi-functional respiratory epithelium which acts as a physical, chemical and immunological barrier to external challenges.^[1] Ciliated epithelial cells form a large part of this barrier and their cilia beat spontaneously in a coordinated fashion to clear mucus and associated debris from the airways. The cilia beat frequency (CBF), beat pattern and the hydration level of the mucus play critical roles in the efficiency of mucociliary clearance.^[2] The integrity of the epithelial barrier is maintained by tight junctions that form between cells and help to restrict particulate invasion. In cases where disease and trauma cause irreparable damage to the airway, reconstruction and regeneration is a challenging clinical problem. Polymeric scaffolds have been proposed, though suitable mechanical compatibility is not matched by biological integration, including epithelial growth.^[3, 4] Such materials have included poly(ϵ -caprolactone)-chitosan composites,^[3] and polyethylene terephthalate-polyurethane composites.^[5] However, new, biocompatible and safe materials permit barrier functions though efficient mucociliary clearance remains elusive.

Several techniques exist to chemically modify implantable materials that could offer benefits over their unmodified forms in terms of biocompatibility. These include treatments with strong acids or bases, corona treatment and flame, irradiation, ultraviolet and laser treatments.^[6] Active screen plasma treatment (ASPT) involves the ionization of a gas in a chamber at low pressure,^[7] where the high energy species, which constitute the plasma, interact with the material to confer surface modification. Fine-tuning of the surface properties is achievable via

careful selection of gas composition, pressure, and electric power.^[8, 9] ASPT is a versatile surface modification technique and can be used for etching,^[10] cleaning,^[11] activation^[12] or deposition^[13] and offers significant advantage over traditional direct plasma treatments as ASPT technology avoids ion bombardment-induced surface damage, has the advantage of preserving the bulk functionality of the original polymer, and is relatively cost- and time-effective. Using ASPT to functionalize biomaterials avoids the use of chemicals which could be hazardous *in vivo*. ASPT has been used to improve the adhesion of endothelial and smooth muscle cells,^[14] fibroblasts^[15, 16] and osteoblasts^[17, 18] to surfaces. Much of the research into ASPT for biomaterials has focussed on the adsorption of globular proteins or growth factors that are appropriate to the native environment.^[19, 20] However, with a greater understanding of protein folding and function, as well as an improvement in the technology used for synthesis, recent work has conjugated specific peptide based functional groups^[21-24] directly onto implantable polymeric materials to control cell migration, attachment, proliferation and differentiation in the immediate vicinity of the implant. These protein mimics are known to promote material-cell interaction via integrin receptors. The attachment of such moieties can improve cellular compatibility.^[25, 26]

The hydrogelating self-assembling fibre (hSAF) system is a *de novo* peptide-based hydrogel system which conjugates functional motifs onto a fibrillar network.^[27] The hSAF network mimics the fibrous extracellular matrix (ECM) and leverages integrin-binding short peptide sequences that control cell attachment, migration and differentiation.^[22, 28] This study explores the hSAF system, in its undecorated form and decorated with RGDS (a fibronectin cell adhesion peptide

sequence), as a platform for human epithelial cell (HEC) differentiation. We use ASPT to enhance the adsorption of hSAF nanofibres onto polyhedral oligomeric silsesquioxane (POSS)-based polymers. Here the POSS polymer is used as surrogate for a range of implantable hydrophobic materials. We combined POSS polymer with poly(carbonate urea) urethane (PCUU) to form POSS-PCUU, a material widely used in clinical and environmental contexts (hydrophobic films,^[29] drug delivery carriers,^[30] nanofillers^[31, 32] fire retardants).^[33] As with most synthetic polymers, the cellular adherence and differentiation on POSS-PCUU has proved disappointing compared to natural scaffolds.^[34, 35] Therefore our overarching aim is to generate a polymeric surface amenable to human nasal epithelial cell (HEC) attachment and differentiation, including ciliation, with consequent enhanced potential for clinical application. Our strategy is to explore the adsorption of hSAF nanofibres^[27] onto POSS-PCUU following surface modification using Air, N₂, H₂, H₂:N₂ and Air:N₂ plasmas. These plasma compositions were specifically selected with the objective of generating amine- and carboxylic acid-rich polymer surfaces conducive to the adsorption of hSAF peptides.

2.0 Materials and Methods

2.1 POSS-PCUU Manufacture and Scaffold Formation

A mixture of 2 g *trans*-cyclohexanechloro-drinisobutyl-silsesquioxane (Hybrid Plastics, USA) and 72 g polycarbonate polyol (2000 MW; Sigma Aldrich, UK) was heated to 130°C before being cooled to 80°C. 18.8 g flake 4,40 - methylene bis(phenyl isocyanate) (Sigma Aldrich, UK) was then added to the mixture before reheating to 70-80°C for 120 mins to form the prepolymer.

156 g dimethylacetamide (DMAC; Sigma Aldrich, UK) was then added slowly and cooled to 35°C creating polyhedral oligomeric silsesquioxane poly(carbonate-urea) urethane (POSS-PCUU) solution which was stored at room temperature.

Scaffolds were formed by adding 20 g 25-53 μm sodium hydrogen carbonate (NaHCO_3 ; Sigma Aldrich, UK) particles (sieved) and 2% (w/w) Tween 20 (Sigma Aldrich, UK) to 19.2 g POSS-PCUU solution. The solutions were mixed and 'degassed' (to remove air bubbles) in a centrifugal mixer (2,000 rpm for 3 mins, Thinky ARE-250, USA). Sheets of POSS-PCUU were formed by pouring the mixed solutions onto 148 x 210 mm glass molds with a $\sim 300\mu\text{m}$ thick autoclave tape perimeter and lowering the mold into a deionized water (DI H_2O) bath to allow polymer precipitation and NaHCO_3 particles to leach out of the scaffold. DI H_2O was replaced 3 times a day (every 3 hours) for 5 days before the polymer was lifted out of the bath, peeled off the glass mold and stored in 70% ethanol (v/v ethanol in water). All scaffolds were washed overnight in DI H_2O before use. For epithelial cell studies the samples were further autoclaved at 121 °C for 20 mins in DI H_2O before use.

2.2 Plasma Treatment of POSS-PCUU

POSS-PCUU scaffolds were ASPT in a Klockner Ionon DC plasma furnace (Klöckner Ionon, Germany), using an active screen set-up (**Figure 1**). Samples were treated on the worktable which was kept at floating potential (i.e. insulated from the cathodic surfaces of the plasma furnace), with a 20 mm distance between the samples and the stainless-steel mesh of the active screen. The chamber was evacuated to a base pressure below 1 Pa and back filled to a

pressure of 75 Pa using the gas mixture selected for the ASPT, namely 100% Air, 100% N₂, 100% H₂, 50% N₂ – 50% H₂ and 50% N₂ – 50% Air). Gas lines were evacuated and purged before each treatment, to eliminate the residual gas from the previous experiment. The electric power applied on the active screen was set to 300 W (300 V and 1 A). Scaffolds were ASPT for 5 mins each on both sides and the temperature kept below 60°C (monitored using a K-type thermocouple inserted in a dummy block).

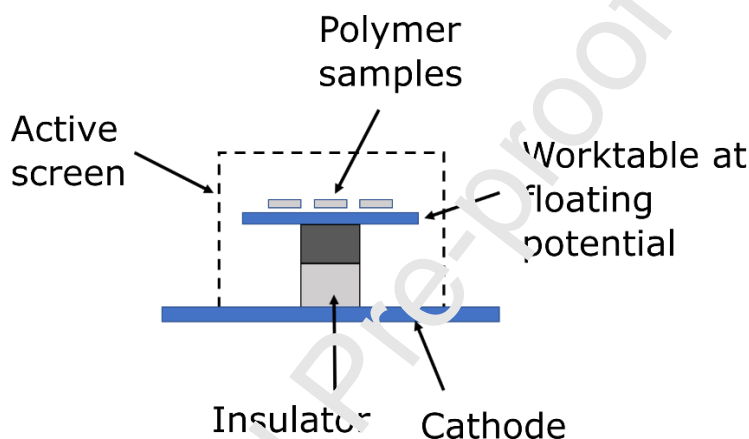


Figure 1: Schematic of the active screen plasma treatment process.

2.3 hSAF Manufacture

All hSAF peptides were manufactured using previously published methods^[24] and chemicals purchased from Sigma Aldrich, UK unless otherwise stated. Briefly, hSAF-p1, hSAF-p1(N₃) and hSAF-p2 were synthesised on a H-Ala-HMPB-ChemMatrix resin (PCAS BioMatrix Inc., Canada) at 0.5 mmol using standard 9-fluorenyl-methoxycarbonyl (Fmoc)-based solid-phase chemistry on a 'Liberty' microwave-assisted peptide synthesizers (CEM, UK) while RGDS (Arg-Gly-Asp-Ser) was synthesised on a Rink Amide-ChemMatrix resin (PCAS BioMatrix Inc., Canada). For hSAF-

p1(N₃) synthesis α -Fmoc- ϵ -azido-norleucine was coupled to hSAF using 2 eq. amino acid, 1.9 eq. O-(7-azabenzotriazol-1-yl)-*N,N,N',N'*-tetramethyluronium hexafluorophosphate and 2.5 eq. *N,N*-diisopropylethylamine while for alkyne modification of RGDS 5 eq. propiolic acid, 6 eq. hydroxybenzotriazole and 4.5 eq. *N,N'*-diisopropylcarbodiimide (Fisher Scientific, UK) were used. Peptide cleavage and the removal of side-chain protecting group was achieved using a trifluoroacetic acid-based (TFA) mixture (TFA:triisopropylsilane:water, 95:2.5:2.5) for 3 hours. The product was then precipitated in cold diethyl ether, centrifuged at 10,000 rpm for 5 mins and the precipitates dissolved in 5 mL of a 1:1 mixture of acetonitrile/water before freeze-drying.

Crude, freeze-dried peptides were purified by reverse-phase high-performance liquid chromatography (HPLC; JASCO, UK) using a Vydac[®] TP C18 column (10 μ m, 22 \times 250 mm) under acidic conditions (buffer A: 0.1% TFA in H₂O; buffer B: 0.1% TFA in acetonitrile). For hSAF-p1, hSAF-p1(N₃) and hSAF-p2 a 20 to 60% v/v buffer B gradient over 60 min was used whilst alk-RGDS was purified using a 5 to 40% v/v buffer B gradient over 60 minutes. Purified peptides were freeze-dried and stored at 4 °C in the dark. Peptides were characterised using previously published matrix-assisted laser desorption/ionization-time of flight mass spectrometry (MALDI-TOF MS), analytical HPLC and UV absorbance methods (data not shown).^[28]

2.4 hSAF Fibre Formation

To form hSAF fibres, on either ASPT POSS-PCUU discs or on transwell inserts (0.4 μ m pore size, 24-well, insert diameter 6.5 mm; Corning, USA), the volume of each polymer disc or transwell

insert was first calculated. Equal volumes of either the hSAF-p1 and hSAF-p2 or hSAF-p1(N₃) and hSAF-p2 were deposited on the surface of the discs/ transwell at 2 mM each in 3-(*N*-morpholino) propanesulfonic acid (MOPS)-buffer (20 mM MOPS, 5 mM sodium acetate, 1 mM EDTA) pH 7.4, giving a final concentration of 1 mM of each peptide. Peptides were left at 4 °C overnight to form fibres. For the hSAF-p1(N₃) and hSAF-p2 samples a mixture of 4 mM CuSO₄, 4 mM ascorbic acid and 2 mM of alk-RGDS was then added to each polymer disc/ transwell and incubated overnight at 4 °C. CuSO₄ catalyst was removed by washing the polymer surface three times with 10 mM EDTA, three times with phosphate buffered saline (PBS; 160 mM NaCl, 3 mM KCl, 8 mM NaHPO₄, 1 mM KH₂PO₄, pH 7.4) for 30 minutes each wash.

2.5 Profilometry

Surface roughness and topography of ASPT POSS-PCUU scaffolds was evaluated through optical profilometry using a DCM3D (Leica Microsystems, UK). Samples were imaged using a 20X objective lens, which corresponded to an analysis window of dimensions 637 µm x 477 µm. Images were analysed using Scanning Probe Image Processor software (Image Metrology, Denmark) to give an average surface roughness; S_a . Each value presented represents the mean of a minimum of five measurements across the surface of each scaffold.

2.6 X-ray Photoelectron Spectroscopy

hSAF deposition on POSS-PCUU was confirmed by analyzing surface composition, specifically the presence of chemical bonding environment, using a K-alpha X-ray Photoelectron Spectrometer (Thermo Fisher Scientific, UK) with a microfocused monochromated Al K α X-ray

source, a spot size of 400 μm and a power of 36 W. Step size was 0.1 eV for individual peaks and 1 eV for a full spectrum over the complete range of binding energies (BEs) and the vacuum pressure in the analysis chamber was $< 10^{-7}$ Pa. Analysed photoelectron peaks include C 1s (BE = 285 eV), N 1s (BE = 400 eV) and O 1s (BE = 531 eV) with three regions measured for each sample. All data were processed using CasaXPS software (Casa Software Ltd., UK). A Gaussian-Lorentzian function was used to fit the data with background subtracted using the Shirley method.

2.7 Contact Angle

The surface wetting behaviour of ASPT polymer was assessed using a DSA 100 Drop Shape Analyzer (Krüss, UK), with DI H₂O adjusted to pH 5, 7 and 9 (using HCl and NaOH solutions) as the analytes. Samples were first critical point dried before 5 μL droplets were deposited on the surface using a flat-ended needle. Data were collected at 20-22 °C and 40-60% relative humidity.

2.8 Atomic Force Microscopy

Acquisition of adhesion data was performed using a NanoWizard II AFM (JPK Instruments, UK) employing a CellHesion module (JPK Instruments, UK), operating in force spectroscopy mode at 18 °C. The sample and cantilever were immersed in aqueous solution in the pH range 5-9, contained within a clean glass Petri dish. Samples were immobilized using double-sided Shintron adhesive tape (Agar Scientific, UK). A rectangular hemispherical-tipped Si cantilever (SD-Sphere-CONT-M-10, NanoWorld, Switzerland) was employed. The length and width of the

cantilever were 450 μm and 50 μm respectively; the tip diameter was 2 μm . The spring constant was 0.42 N/m, calibrated according to the method reported by Bowen *et al.*[36] In aqueous solution at pH 5-9 the cantilever probe will present an anionically charged surface. Data were acquired by driving the fixed end of the cantilever at a velocity of 2.5 $\mu\text{m/s}$ towards the sample surface, whilst monitoring the deflection of the free end of the cantilever. A maximum compressive load of 10 nN was applied to the surface during data acquisition. Vertical deflection and z-axis displacement data were recorded at a frequency of 10 kHz. A grid of 100 force-displacement curves were acquired for each sample, liquid combination, equally spaced over an area of 100 μm x 100 μm . Force-displacement data were analysed using JPK Data Processing software (JPK Instruments, UK).

2.9 Field Emission Scanning Electron Microscopy

The microstructure of ASPT POSS-PCU polymer samples with hSAFs was evaluated by field emission scanning electron microscopy (FEG-SEM, Jeol JSM, 7401F, Jeol, UK). The samples were first fixed in 4% paraformaldehyde (in phosphate buffered saline; Alfa Aesar, UK) for $\frac{1}{2}$ hr before dehydration in graded ethanol 20%, 30%, 50%, 70%, 90% and 100% v/v ethanol in water for $\frac{1}{2}$ hr each. The ethanol was then exchanged for liquid CO_2 and the samples were critical point dried at 1040 psi and 32 $^\circ\text{C}$ in a critical point dryer (Electron Microscopy Sciences, UK). Dried specimens were mounted onto stubs and ion beam-coated with 4 nm of platinum (Quorum Scientific High Vacuum Sputter Coater Q150T, Quorum Technologies, UK). Micrographs of polymer and peptides were imaged by secondary electron detection at an accelerating voltage of 5 kV and a working distance of 7 mm. Stereo anaglyphs were created by

merging two images of the same sample area taken at no tilt and a 10° tilt using Stereo Works 1.1 software (<https://sourceforge.net/projects/stereoworks/>). Three samples were analysed for each group and five stereo anaglyphs were taken per sample.

2.10 Primary Cell Culture from Nasal Brush Biopsies

For cell culture studies transwell inserts (0.4 µm pore size, 24-well, insert diameter 6.5 mm; Corning, USA) were first coated with either the undecorated hSAF or RGDS-decorated hSAFs as described in Section 2.4 or collagen (1% w/v in PBS, incubation for 1hr followed by triple wash with water, Collagen I (rat tail, Corning, USA)).

Human respiratory epithelial cell cultures were derived from nasal brushing from healthy females (age 30-40). Ethical approval was obtained through the Living Airway Biobank (REC reference 14/NW/0128) and UCL Research Ethics (reference 4735/001). The HECs were expanded in co-culture with mitomycin-inactivated 3T3-J2 fibroblasts as previously described.^[37] HECs were cultured at 37°C and 5% CO₂ with three changes of medium per week (every 2-3 days) until confluent. Expansion medium contained: Dulbecco's Modified Eagle's Medium (DMEM, Gibco; 41966, USA) and F12 (Gibco; 21765, USA) in a 3:1 ratio with 1X penicillin/streptomycin (Gibco; 15070, USA) and 5% (v/v) Fetal Bovine Serum (Gibco; 10270, USA) supplemented with 5 µM Y-27632 (Cambridge Bioscience; Y1000, UK), 25 ng/mL hydrocortisone (Sigma Aldrich; H0888, USA), 0.125 ng/mL Epidermal Growth Factor (Sino Biological; 10605, China), 5 µg/mL insulin (Sigma Aldrich; I6634, USA), 0.1 nM cholera toxin

(Sigma Aldrich; C8052, USA), 250 ng/mL amphotericin B (Fisher Scientific; 10746254, UK) and 10 µg/mL gentamycin (Gibco; 15710, USA).

At confluency, basal cells were separated from feeder cells using differential trypsinization; first, an incubation with 0.05% (v/v) trypsin/EDTA (Sigma Aldrich, USA) to remove fibroblasts followed by TripLE (Life Technologies, USA) incubation to collect HECs.^[38] Cells were seeded on previously prepared semi-permeable membrane supports: 0.5 × 10⁶ cell per transwell (0.4 µm pore size, 24-well, insert diameter 6.5 mm; Corning, USA) in submerged culture in the expansion medium. After 48 hours, apical medium was removed and basolateral medium replaced with (air liquid interface) ALI-medium, consisting of 50% (v/v) DMEM and 50% (v/v) PromoCell's Airway Epithelial Cell Growth Medium (PromoCell, Germany) supplemented with 1 µM additional retinoic acid (Sigma Aldrich, USA), 1X penicillin/streptomycin (Gibco; 15070, USA). Basolateral medium was exchanged three times per week (every 2-3 days) for 28 days.

2.11 Immunofluorescence

Differentiated HECs were fixed directly on the transwell membrane by incubation in 4% (v/v) paraformaldehyde (Sigma Aldrich, USA) at room temperature for 30 minutes, fixative was then replaced with phosphate buffered saline (PBS) and cells stored at 4°C in PBS until required. Cells were blocked and permeabilised using blocking buffer (3% v/v Bovine Serum Albumin in PBS containing 0.01% v/v Triton X-100) at room temperature for 1 hour. Cells were stained overnight with primary antibodies (anti-beta tubulin, Abcam; ab15568, UK, 1:100 in 1% v/v BSA in PBS). Cells were washed 3 times in PBS for 5 minutes and secondary antibody (in 1% v/v BSA

in PBS; anti-rabbit AlexaFluor 488, Abcam, ab150077, UK, 1:250 in 1% BSA in PBS) was applied for 2 hours at room temperature followed by incubation with phalloidin for F-actin staining (Phalloidin-iFluor 555 Reagent-Cytopainter Abcam, ab176756, UK, 1:2000 in 1% v/v BSA in PBS). Hoechst 33258 staining solution (Sigma Aldrich, USA) was then added for 20 minutes at room temperature as a nuclei counterstain prior to imaging. Cells were mounted in 80% v/v glycerol, 3% v/v n-propylgallate (in PBS) mounting medium and images were obtained using an inverted Zeiss LSM 710 confocal microscope (Zeiss, Germany) using a 20X objective (63X for z-stacks).

2.12 Transepithelial Electrical Resistance (TEER)

TEER values were measured using an EVOM2 resistance meter (World Precision Instruments, UK) and Chopstick Electrode Set STX2 (World Precision Instruments, UK). 100 μ L of PromoCell basal medium was added to the apical surface of the transwell and the electrode placed between the apical and basolateral compartments. Readings were taken from three independent transwells once per week for four weeks.

2.13 High-video Microscopy, Ciliary Beat Frequency and Ciliary Dyskinesia

Differentiated ciliated cells were observed using an inverted microscope system (Nikon Ti-U, Japan) using a 20X objective. At least 20 top-down videos per donor were recorded and ciliary beat frequency (CBF) was determined using the ImageJ plugin CiliaFA.^[39] The ciliated epithelium was removed from the transwell insert by gentle scraping with a spatula in transport media (Medium 199, Life Technologies, #22340020, USA) containing 100 U/mL penicillin, 100 μ g/mL streptomycin (Gibco, #15290026, USA), 25 μ g/mL amphotericin B and 20.5 μ g/mL sodium

deoxycholate (Gibco, #15290018, USA) and placed on glass slides covered by a coverslip. Beating cilia were recorded on a warmed stage at 37°C using a digital high-speed video camera (Motion Pro 4x; IDT, USA) at a rate of 500 frames/second using a 100X objective. The percentage of cells which displayed dyskinesia, an abnormal cilia beat pattern, was calculated using the number of dyskinetic ciliated cells relative to the total number of motile ciliated cells.

2.14 Statistical Analysis

All data are presented as “mean \pm standard error of mean (SEM)”. The mean value differences between groups, and whether the differences were significant, were determined by a two-way Analysis of Variance (ANOVA) with a post hoc Tukey HSD (honestly significant difference) test. The significance level was set at $p < 0.05$.

3.0 Results

3.1 Effect of Plasma Treatment on Polycarbonate Urethane-modified Silsesquioxane

The surface topography of polymers before and after ASPT exhibited some variation (**Figure 2A**), though this was somewhat confounded by differences in surface roughness on each side examined (i.e. side 1 or side 2; **Figure 2B**). Differences between polymer side 1 and side 2 have previously been attributed to the coagulation method used, during which one side was in

contact with a smooth glass surface.^[34] Side 2 (the non-contact side, presented at the air-liquid interface during coagulation) showed more than double the roughness compared to side 1, across all ASPT samples. However, no significant differences were measured on the non-contact side (side 2) for any of the ASPT samples compared to the control samples before ASPT.

The polymer surface composition was significantly modified by each ASPT investigated. Compared to the control decreases in the atomic % (at%) C and Si were identified from XPS measurements along with increases in at% O (**Figure 2C**). An improved wettability of the polymer surface was evidenced by decreased contact angle values recorded at pH 5, 7 and 9 for all ASPTs (**Figure 2D**). The adhesion energy between the polymer surface and the probe surface was significantly reduced for all ASPTs except ASPT (Air) (**Figure 2E**). The adhesion of the ASPT (N₂) and ASPT (Air:N₂) surfaces increased with increasing pH, whereas the adhesion of the ASPT (H₂) and ASPT (H₂:N₂) surfaces decreased with increasing pH. The probe surface is negatively charged at pH > 4. Therefore, ASPT (N₂), ASPT (H₂:N₂) and ASPT (Air:N₂) surfaces appear to present an overall positive charge, likely due to the formation of amine (NH₂) functional groups.^[16]

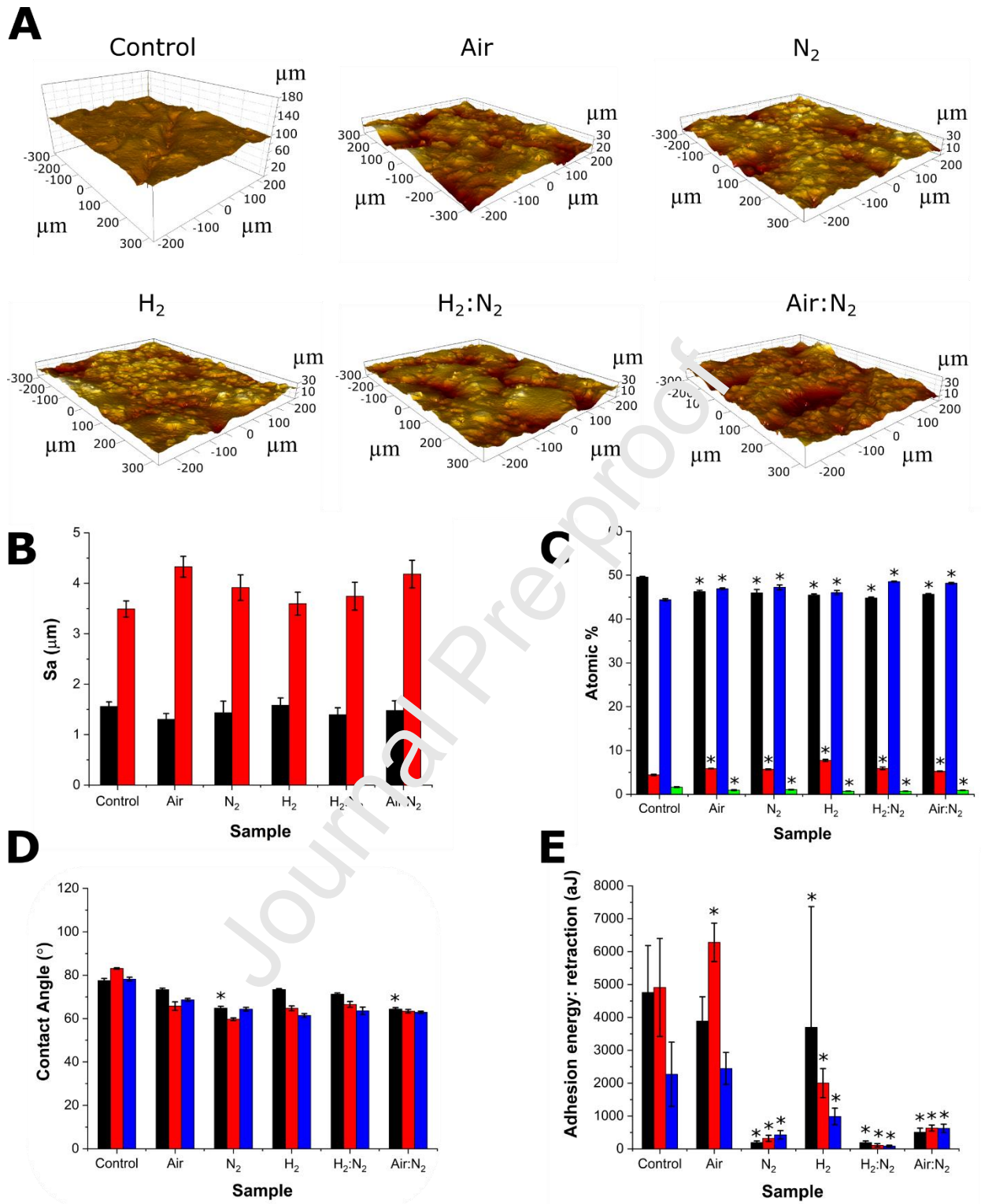


Figure 2: Physicochemical characterisation of plasma treated polymer surfaces. Representative 3-dimensional images of surfaces for control, ASPT (Air), ASPT (N₂), ASPT (H₂), ASPT (H₂:N₂) and ASPT (Air:N₂) polymers (A) with quantification of polymer surface roughness on side 1 (black) and side 2 (red) in μm (B). Changes to C (black), N (red), O (blue) and Si (green) chemistry on polymer surface (C) and the effect of changing polymer surface chemistry on the water contact angle (D). Effect of plasma treatment on adhesion energy (E) at pH 5 (black), pH 7 (red) and pH 9 (blue). * represents statistically significant difference between the sample and the control ($p < 0.05$).

3.2 Adsorption of α -Helical Peptides on Plasma-treated Polymer

hSAF peptides were adsorbed onto each of the ASPT polymer surfaces and the change in surface composition, indicative of peptide adsorption, was measured using X-ray photoelectron spectroscopy. An increase in at% N content was observed for all samples, suggesting a new surface layer was present covering the Si-containing polymer (**Figure 3A**). Significant changes in at% C and O were also noted between ASPT samples and ASPT samples with adsorbed hSAF (**Figure S2**).

Analysis of the C 1s photoelectron peaks, specifically the C-C, C-O, C-N, R-C=O and π - π^* composition, showed a decrease in the proportion of aliphatic and aromatic C-C bonds and an increase in C-O, C-N and/or R-C=O bonds, indicative of amino acids and therefore hSAF adsorption. Representative spectra are shown in **Figure 3B** for samples treated with ASPT (Air);

all other spectra are shown in **Figure S1A and S1B**). The percentage composition of each species between samples post-plasma and post-plasma with hSAF adsorption are presented in **Figure S1C and S1D**.

While hSAF nanofibres do not adsorb onto the surface of the control polymers (**Figure 3C**; control), adsorbed peptides were observed on all ASPT samples via electron microscopy (images of all ASPT surfaces before hSAF adsorption are shown in **Figure S3**). The coverage of nanofibres across the polymer surface did not vary noticeably between ASPTs.

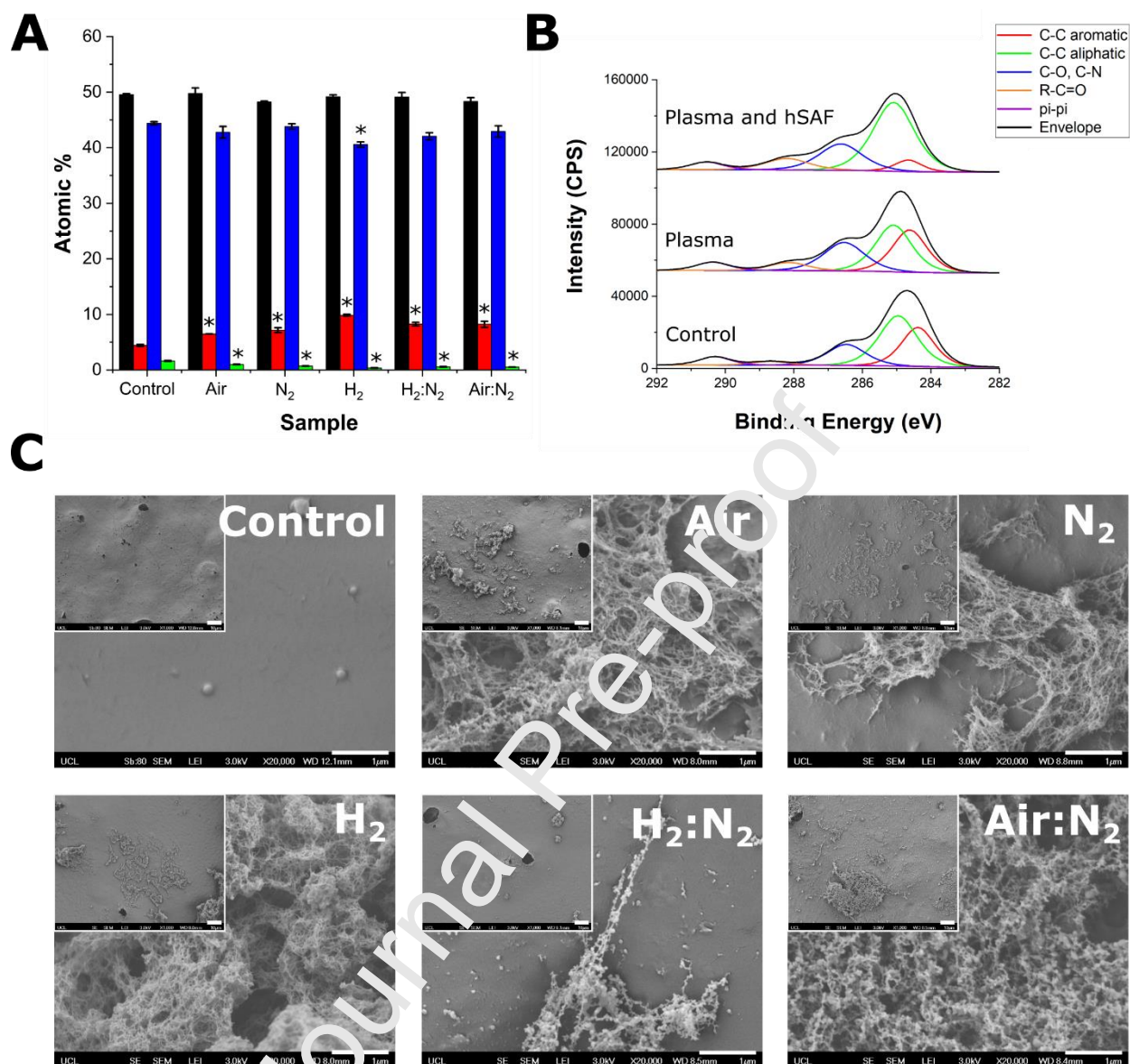


Figure 3: hSAF adsorption on ASPT polymers. Changes to C (black), N (red), O (blue) and Si (green) chemistry on polymer surface (A) with representative spectra showing intensity of aromatic and aliphatic C-C, C-O, C-N, R-C=O and π - π^* post-plasma and post-plasma with hSAF adsorption (B). Representative electron micrographs show distribution of hSAF nanofibres adsorbed onto ASPT samples (C: inset) and the morphology of the adsorbed fibrous network (C: main images). Scale bar for C: 1 μ m. * represents statistically significant difference between the sample and the control ($p < 0.05$).

3.3 *In Vitro* Differentiation of Primary Respiratory Epithelial Cells on Plasma-treated Polymer

Cultured primary epithelial cells from nasal brushings form a structured ciliated epithelium after four weeks *in vitro* at an air-liquid interface (ALI). We used previously developed methodology to expand nasal epithelium cells from a single brushing^[38] and optimised these methods for culturing cells at ALI.^[40-42] Specifically, at ALI the HECs fully differentiated on collagen, undecorated hSAF and RGDS-decorated hSAF hydrogels (**figures 4 and 5**). Cells were positive for 4',6-diamidino-2-phenylindole (DAPI), F-actin and β -tubulin on all three sample types with no obvious differences in expression between the collagen control and peptide-based hydrogels (**Figure 4A-4D**). Transepithelial resistance (TEER) measurements, as an indicator of barrier function, also showed evidence of tight junctions forming on all sample types (**Figure 4E**). Junctions with greater integrity than the collagen control were recorded on undecorated hSAF hydrogels after 14 days in culture, although by day 28 no significant difference was measured between hSAF undecorated, RDGS-decorated and the collagen hydrogels.

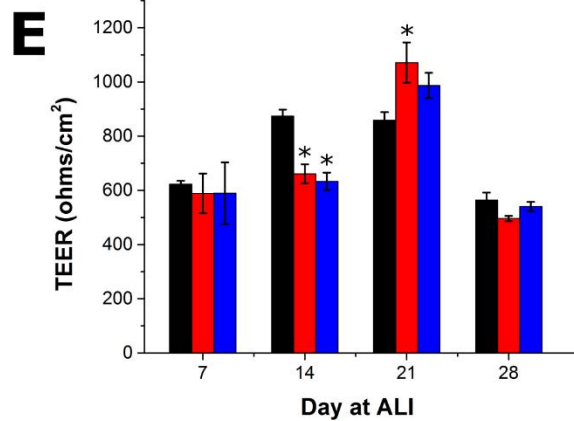
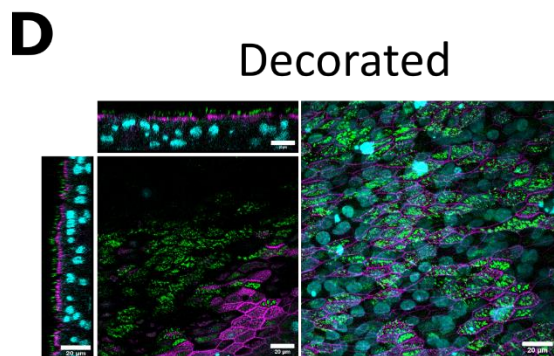
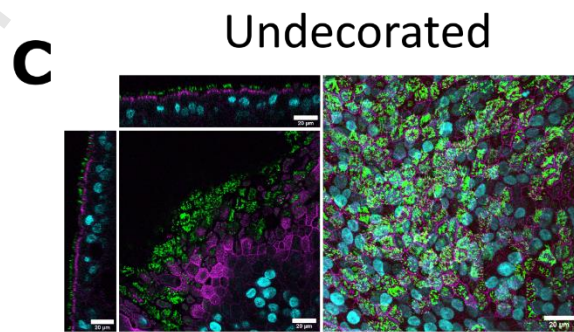
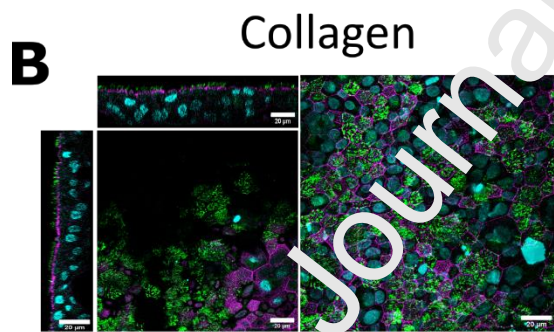
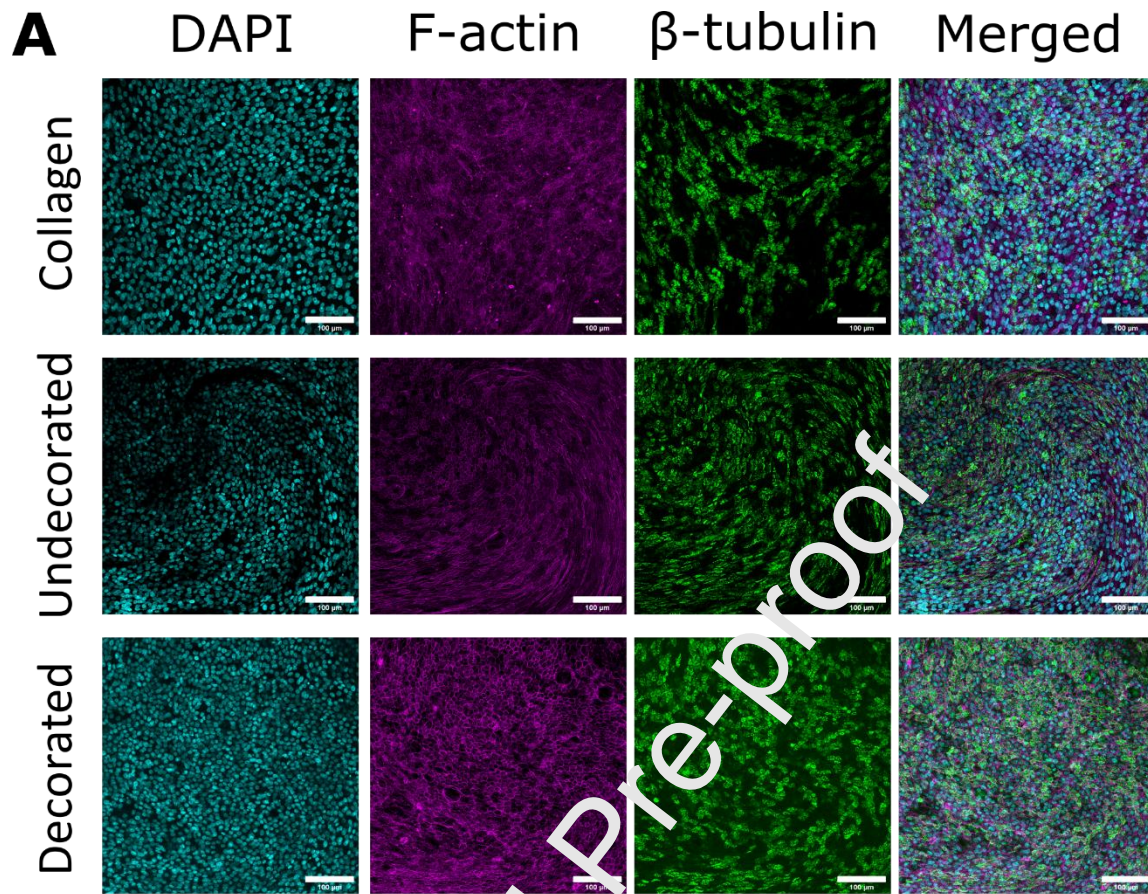


Figure 4: Epithelial differentiation on collagen and peptide-based hydrogels. Expression of DAPI (cyan), F-actin (magenta) and β -tubulin (green) on cells cultured on collagen, undecorated hSAFs and RGDS-decorated hSAFs (A). Z-stack compilations for the same markers are shown for collagen (B), undecorated hSAFs (C) and RGDS-decorated hSAFs (D). Transepithelial resistance for collagen (black), undecorated hSAFs (red) and RGDS-decorated hSAFs (blue) is presented over 28 days. * represents statistically significant difference between the sample and the collagen control ($p < 0.05$). Scale bar for A: 100 μm ; B-D: 20 μm .

Ciliated cells were observed on all hydrogel types (**Figure 5A-5C**) across the entire surface of the sample (**Figure 5A**). Some differences were observed in cell morphology (**Figure 5B**) although this did not affect cilia morphology or orientation (**Figure 5C**). Cilia activity was detected and recorded in all cultures using high-speed video microscopy (**Video S1-S3**) to further test the functionality of the differentiated cells. The cilia beat spontaneously on all hydrogel samples post-ALI. Ciliary dyskinesia, an abnormal cilia beat (**Figure 5D**), was low across all materials (**Table S1**).^[43, 44] Cilia beat frequency was in the range 10-11 Hz (**Figure 5D**), with no significant differences between gel types. These values are within the normal range observed in the human respiratory tract (10-15 Hz).^[45, 46]

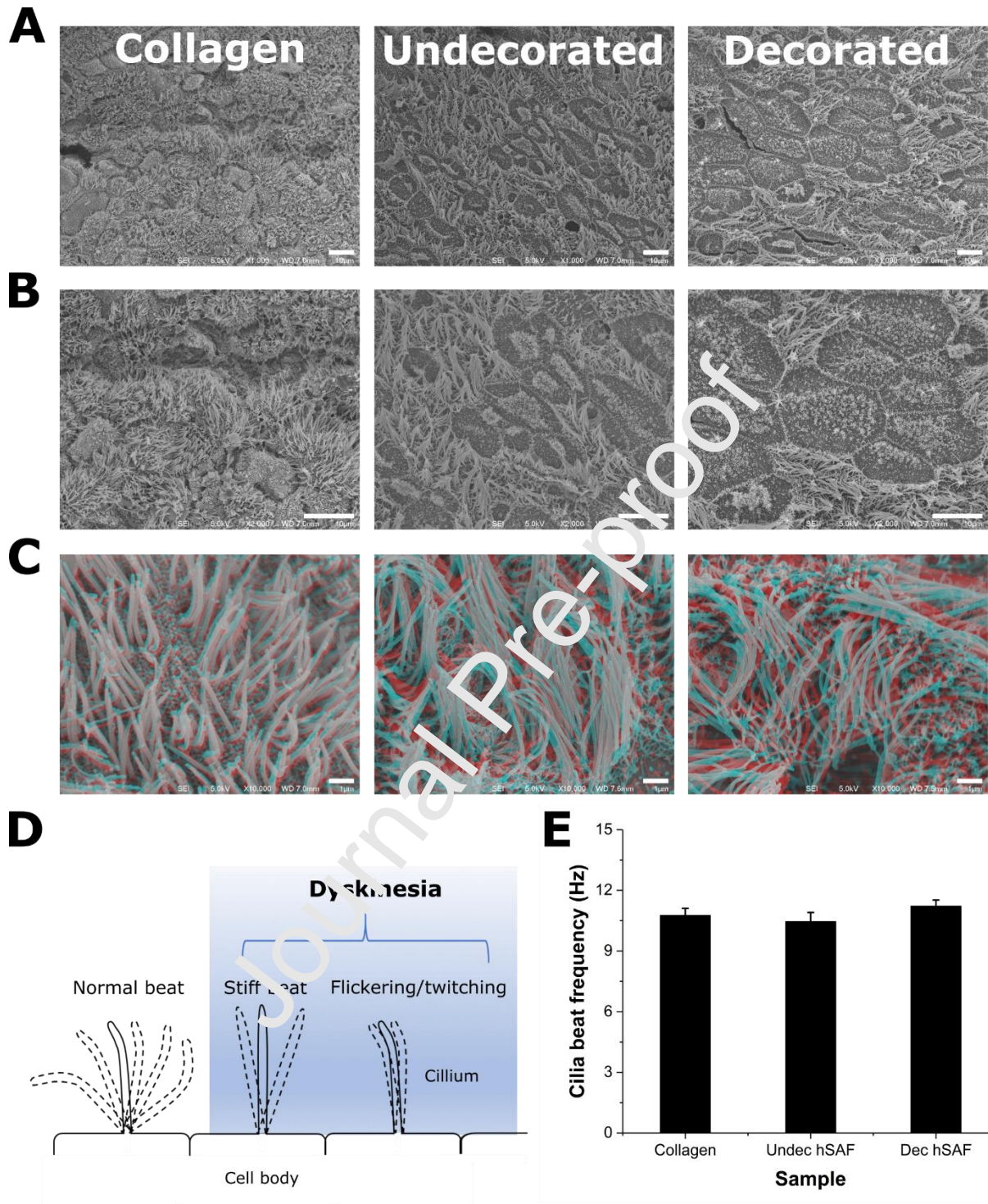


Figure 5: Ciliation of HECs on collagen and peptide-based hydrogels. Representative scanning electron micrographs show the distribution of ciliated HECs across the sample surface (A) and the tight junctions formed between cells (B). Stereo anaglyphs show cilia orientation on each sample type (C) after 28 days of culture. Cilia beat pattern was assessed for dyskinesia (D) and their frequency recorded from video analysis for collagen, undecorated hSAFs and RGDS-decorated hSAFs (E). Scale bar for A-B: 10 μm ; C: 1 μm .

4.0 Discussion

The airway respiratory epithelium is a physical barrier preventing debris from passing through to the internal environment while also expelling particulate-trapping mucus up the airway via ciliated epithelial cells. Polymers have previously been used to replace lost airway structure and integrity though they have been unable to fully restore epithelial functionality. We investigated plasma treatment and α -helical peptide adsorption as a strategy to promote functional differentiation of airway epithelial cells.

All ASPTs investigated promoted the adsorption of peptide nanofibres onto POSS-PCUU. The hydrogels supported the growth and differentiation of HECs capable of generating a ciliated epithelium with actively beating cilia. The functional restoration of cilia in cells isolated from patient nasal brushings, and grown in a chemically controllable environment, presents an interesting addition to traditional collagen-based studies. Collagen, as the predominant component of native ECM,^[47] provides a suitable environment for HEC attachment,

proliferation and differentiation.^[48] However, compositional variation between batches of native collagen presents challenges absent with our peptide nanofibres (the *de novo* designed hSAF system). The hSAF hydrogels have been used to create chemically and physically tunable environments for cell culture^[22, 27, 28] presenting a powerful tool for manufacturing biocompatible materials. Here, hSAFs supported the attachment and proliferation of HECs with a well-organized multistratified epithelium and maintain their function as a physical barrier for several weeks; previous work also showed that these cultures preserve disease-specific phenotypes/characteristics and cell composition (ciliated, goblet, basal cells) (unpublished). Together with the fact that this technique allows the *in vitro* expansion of respiratory epithelial cells from a single patient nasal brushing, these findings offer a potential route to generating autologous cultured mucosal grafts that will not reject in patients. This is important due to outstanding concerns and barriers to the routine use of pluripotent and embryonic stem cells for regeneration.^[49] When combined with implantable polymers the hSAFs promote specific cell responses with implications for reducing chronic inflammation around medical devices.^[50]

Generating a mechanistic understanding of how the peptides interact with the plasma-modified polymer surface is non-trivial. Consideration must be given to how the peptides interact with each other in the vicinity of the polymer surface. Upon mixing the two hSAF peptides, hSAF-p1 and hSAF-p2, 'sticky-ended' dimers attach end-to-end onto other dimers until the peptides are depleted; thus forming fibres. In this study the peptide solutions were premixed before being introduced to the ASPT surface, and during this time dimers are already forming in solution and propagating into fibres. Therefore, peptide-peptide interactions occur in advance of peptide-

surface interactions. The adsorption of peptides and globular proteins onto surfaces is driven by van der Waals, hydrophobic, and electrostatic interactions.^[51] Surfaces that are non-polar, exhibit high surface energy or present charged moieties, and can cause conformational changes in those regions of a peptide or globular protein near to the surface.^[52, 53] Cooperative adsorption, overshooting adsorption kinetics, aggregation^[54] and irreversible structural changes that could inactivate, or reorient, the sites of proteins which interact with cells have also been reported.^[55]

The hydrophobic regions of globular proteins exclude water from the protein-surface interface, making it entropically unfavorable for the interface to be rewetted.^[56] As such, the likelihood of protein desorption from a hydrophobic surface is less than the likelihood of desorption from a hydrophilic surface. Our studies show that the control polymer, which has not received plasma treatment, presents the most hydrophobic surface yet shows no evidence of peptide adsorption. The hydrophobic region of the hSAF peptides (containing isoleucine and leucine) is buried within the core of the dimer, with the nanofibre surface presenting less hydrophobic amino acids (primarily alanine), as well as charged residues (lysine and glutamic acid). Therefore, the adsorption of hSAFs to the hydrophobic polymer surface was not anticipated, nor was it observed.

However, the hydrophobicity/ wettability of the polymer surface alone is insufficient for determining the likely behaviour of a polymer-peptide system; this is particularly true when considering the possibility of peptide structural rearrangements. Our data indicate that the

fibres may be 'clustering'. Clustering is thought to occur either due to (i) positive cooperative adsorption, in which the size of the initial adsorption cluster relates directly to the binding affinity of the peptides still in solution,^[57] or (ii) the aggregation of the peptides in solution which then bind to the polymer surface.^[58] In both cases the implication is that over time there is potential for the cluster size to grow and, therefore, improve the distribution of peptide across the polymer surface.^[54] Although not investigated for the current study, it would be useful to explore time-dependent growth in solution, simultaneous with surface adsorption, in an effort to improve the distribution of adsorbed peptide on polymers. These studies may also be impacted by the solvent system in which the peptides are dissolved.

Weidner *et al.* showed that an interfacial layer of structured water can form between α -helical peptides and hydrophobic fluorocarbons.^[55] For the hSAF system, where MOPS buffer is currently used, the possibility that other dissolved species can act as 'bridging agents' should be explored. Electrostatic repulsion between peptides are minimised at the isoelectric point allowing higher packing densities on the surface. Adsorption rates are high when protein and substrate bear opposite charges since electrostatic attractions accelerate the migration towards the surface. However, the total mass load is generally observed to be maximized at the isoelectric point.^[39-41] The isoelectric point (pI) of the hSAF peptides is 6.93, meaning that our nanofibres exhibit zero net charge in solution at pH 7. Positively and negatively charged regions will be present on the exterior of nanofibres, due to amine (NH₂) and carboxylic acid (COOH) moieties, from lysine and glutamic acid respectively. At pH 7, we hypothesize that the adhesion

of nanofibres to the ASPT surface is likely to result from electrostatic interactions between the positively charged surface and the δ -COOH moieties on the hSAFs.

Establishing which functional groups are generated on the polymer surface via ASPT would permit the development of strategies for controlling peptide adsorption. Due to the chemical complexity of POSS-PCUU, it is difficult to quantify the type of functional groups generated during the ASPT via XPS analysis. However, the pH-responsive nature of the newly created surface suggests that NH_2 and COOH moieties are likely to be presented. This is supported by the increased at% N observed on the ASPT surfaces, as well as the decrease in at% Si, suggesting that the Si-containing POSS cores may now be further away from the polymer surface. Thus, ascertaining the optimal conditions for hSAF nanofibre adsorption on the POSS-PCUU polymer surface requires measurement of: (i) the rate at which fibre assembly occurs in solution; and (ii) the rate at which peptides adsorb to the polymer surface (the adsorption isotherm). Future efforts will explore utilizing the tryptophan amino acid present in the hSAF backbone for monitoring solution and surface concentration of the peptides. Establishing unambiguously which functional groups are presented at the ASPT polymer surface would substantially inform this work.

The adsorption studies presented initiate understanding of complex behaviour, specifically the adsorption phenomena, of these peptides on charged/-uncharged surfaces. Systematic studies could include, though would not be limited to: molecular dynamics simulations as predictive models for peptide behaviour in different environments; mathematical modelling of gelation and adsorption kinetics; imaging techniques to explore peptide distribution on surfaces; and

neutron reflectometry to measure the thickness of the adsorbed peptide layer. However, all five ASPTs explored in our study generate a surface amenable to hSAF nanofibre adsorption, which in turn promote functional HEC differentiation. Where regeneration of a ciliated epithelium would have advantages in a clinical setting, this strategy could be used to chemically modify implantable polymers towards a more functional epithelium.

5.0 Conclusion

Our results show that Air, N₂, H₂, H₂:N₂ and Air:N₂ plasma treatments support the adsorption of *de novo* α -helical peptide fibres onto silsesquioxane based polymers. The hSAF peptide system promotes the attachment, proliferation and differentiation of human nasal epithelial cells with cilia observed on the surface of both undecorated and RGDS-decorated hSAF hydrogels after 28 days and at an air-liquid interface. Inter-cellular tight junctions and cilia beating at a normal frequency indicate that the manufactured peptide materials offer a controllable environment that promote a functional response in epithelial cells. This system could be used to generate autologous cultured mucosal grafts with improved integration that will not reject in patients and functional polymers with reduced chronic inflammation around medical devices in the therapy of airway disorders.

Acknowledgments

This research was supported by the Engineering and Physical Sciences Research Council (EP/R02961X/1). S.C.G. and H.D. received support from EC FIBASPEC (GA604248). D.C. and C.O.C. received support from Action Medical Research (GN2336) and Great Ormond Street Hospital Charity and Sparks National Funding (V4818). This work is partly funded by the NIHR GOSH BRC. M.A.B. is supported partially by NIHR Senior Investigator Award (NIHR201360). The views expressed are those of the authors and not necessarily those of the NHS, the NIHR or the Department of Health. D.A.S. was supported by the BBSRC South West Biosciences Doctoral Training Partnership (BB/J014400/1 and BB/M009122/1). D.N.W. held a Royal Society Wolfson Research Merit Award (WM140008). The funders had no role in study design; in the collection, analysis and interpretation of data; in the writing of the report; and in the decision to submit the article for publication. The authors are grateful to Dr. Anwen Bullen at University College London Ear Institute for insights and discussions on scanning electron microscopy, the National EPSRC XPS Users' Service (NEXUS) at Cardiff University, an EPSRC Mid-Range Facility, for access to X-ray photoelectron spectroscopy; and University College London Department of Surgery for their support in producing the polymer. We thank BrisSynBio for access to the CEM Liberty Blue peptide synthesizer at the University of Bristol.

References

- [1] E. Waltl, R. Selb, J. Eckl-Dorna, C. Mueller, C. Cabauatan, T. Eiwegger, Y. Resch-Marat, K. Niespodziana, S. Vrtala, R. Valenta, V. Niederberger, *Sci. Rep.* **2018**, *8*, 9688.
- [2] S. Ganesan, A. Comstock, U. Sajjan, *Tissue Barriers* **2013**, *1*, e24997.
- [3] C. Mahoney, D. Conklin, J. Waterman, J. Sankar, N. Bhattarai, *J. Biomat. Sci.* **2016**, *27*, 611.

- [4] L. Brizielli, G. Perale, Engineering airways, in: G. Perale, J. Hilborn (Eds.), *Bioresorbable Polymers for Biomedical Applications: From Fundamentals to Translational Medicine*, Woodhead Publishing, Manno, Switzerland, **2017**, pp. 543.
- [5] C. Best, V. Pepper, D. Ohst, K. Bodnyk, E. Heuer, E. Onwuka, N. King, R. Strouse, J. Grischkan, C. Breuer, J. Johnson, T. Chiang, *Int. J. Paediatr. Otorhinolaryngol.* **2017**, *104*, 155.
- [6] L. Karam, C. Jama, P. Dhulster, N.-E. Chihib, *J. Mater. Environ. Sci.* **2013**, *4*, 798.
- [7] J. Hall, C. Westerdahl, A. Devine, M. Bodnar, *J. Appl. Polym. Sci.* **1969**, *13*, 2085.
- [8] L. Tao, X. Duan, C. Wang, X. Duan, S. Wang, *Chem. Comm.* **2015**, *51*, 7470.
- [9] C. Chen, B. Liang, D. Lu, A. Ogino, X. Wang, M. Nagatsu, *Carbon* **2010**, *48*, 939.
- [10] X. Dong, H. Li, M. Chen, Y. Wang, Q. Yu, *Clin. Plasma Med.* **2015**, *3*, 10.
- [11] B.-O. Aronsson, J. Lausmaa, B. Kasemo, *J. Biomed. Mater. Res. A* **1997**, *35*, 49.
- [12] Q. Chen, L. Dai, S. Huang, A. Mau, *J. Phys. Chem. B* **2001**, *105*, 618.
- [13] D. Hegemann, H. Brunner, C. Oehr, *Nucl. Instrum. Methods Phys. Res. B* **2003**, *208*, 281.
- [14] Q. Cheng, B.-P. Lee, K. Komvopoulos, Z. Yan, S. Li, *Tissue Eng. Part A* **2013**, *19*, 1188.
- [15] A. Borges, L. Benetoli, M. Licínio, V. Zoldan, M. Santos-Silva, A. Pata, M. Debacher, V. Soldi, *Mater. Sci. Eng. C* **2013**, *33*, 1315.
- [16] G. Kaklamani, J. Bowen, N. Mehrban, H. Dong, L. Grover, A. Stamboulis, *Appl. Surf. Sci.* **2013**, *273*, 787.
- [17] M. Domingos, F. Intranuovo, A. Gloria, R. Gristina, L. Anichini, P. Bártolo, P. Favia, *Acta Biomater.* **2013**, *9*, 5997.
- [18] X. Fu, R. Sammons, I. Bertóti, M. Jenkins, H. Dong *J. Biomed. Mater. Res. B Appl. Biomater.* **2011**, *100B*, 314.
- [19] T. Haddad, S. Noel, B. Liberelle, R. El Ayoubi, A. Ajji, G. De Crescenzo, *Biomaterials* **2016**, *6*, 2159.
- [20] T. Ham, M. Farrag, N. Leipzig, *Acta Biomater.* **2017**, *53*, 140.
- [21] K. Uto, J. Tsui, C. DeForest, D.-H. Kim, *Prog. Polym. Sci.* **2017**, *65*, 53.
- [22] N. Mehrban, B. Zhu, F. Tamagnini, F. Young, A. Wasmuth, K. Hudson, A. Thomson, M. Birchall, A. Randall, B. Song, D. Woolfson, *ACS Biomater. Sci. Eng.* **2015**, *1*, 431.
- [23] Y. Jiang, J. Chen, C. Deng, E. Suuronen, Z. Zhong, *Biomaterials* **2014**, *35*, 4969.
- [24] N. Mehrban, E. Abelardo, A. Wasmuth, K. Hudson, L. Mullen, A. Thomson, M. Birchall, D. Woolfson, *Adv. Health. Mater.* **2014**, *3*, 1387.
- [25] E. Masaeli, P. Wieringa, M. Mouched, M. Nasr-Esfahani, S. Sadri, C. van Blitterswijk, L. Moroni, *Nanomed-Nanotechnol.* **2017**, *10*, 1559.
- [26] B. Richter, V. Hahn, S. Lertes, T. Claus, M. Wegener, G. Delaittre, C. Barner-Kowollik, B. M, *Adv. Mater.* **2017**, *29*, 1604342.
- [27] E. Banwell, E. Abelardo, D. Adams, M. Birchall, A. Corrigan, A. Donald, M. Kirkland, L. Serpell, M. Butler, D. Woolfson, *Nat. Mater.* **2009**, *8*, 596.
- [28] N. Mehrban, E. Abelardo, A. Wasmuth, K. Hudson, L. Mullen, A. Thomson, M. Birchall, D. Woolfson, *Adv. Health. Mater.* **2014**, *3*, 1387.
- [29] J. Mabry, A. Vij, S. Iacono, B. Viers, *Angew. Chem.* **2008**, *120*, 4205.
- [30] C. McCusker, J. Carroll, V. Rotello, *Chem. Comm.* **2005**, *8*, 996.
- [31] M. Joshi, B. Butola, *J. Macromol. Sci. C* **2004**, *44*, 389.
- [32] Y. Xue, Y. Liu, F. Lu, J. Qu, H. Chen, L. Dai, *J. Phys. Chem. Lett.* **2012**, *3*, 1607.
- [33] W. Zhang, X. Li, X. Guo, R. Yang, *Polym. Degrad. Stab.* **2010**, *95*, 2541.
- [34] N. Mehrban, J. Bowen, A. Tait, A. Darbyshire, A. Virasami, M. Lowdell, M. Birchall, *Mater. Sci. Eng. C* **2018**, *92*, 565.
- [35] K. Wismayer, N. Mehrban, J. Bowen, M. Birchall, *J. Laryngol. Otol.* **2019**, *133*, 135.
- [36] J. Bowen, D. Cheneler, D. Walliman, S. Arkless, Z. Zhang, M. Ward, M. Adams, *Meas. Sci. Technol.* **2010**, *21*, 115106.

- [37] R. Hynds, C. Butler, S. Janes, A. Giangreco, *Methods Mol. Biol.* **2019**, 1576, 43.
- [38] C.R. Butler, R.E. Hynds, K.H. Gowers, H. Lee Ddo, J.M. Brown, C. Crowley, V.H. Teixeira, C.M. Smith, L. Urbani, N.J. Hamilton, R.M. Thakrar, H.L. Booth, M.A. Birchall, P. De Coppi, A. Giangreco, C. O'Callaghan, S.M. Janes, *Am. J. Respir. Crit. Care Med.* **2016**, 194, 156.
- [39] C. Smith, J. Djakow, R. Free, P. Djakow, R. Lonnen, G. Williams, P. Pohunek, R. Hirst, A. Easton, P. Andrew, C. O'Callaghan, *Cilia* **2012**, 1, 2046.
- [40] R.A. Hirst, C.L. Jackson, J.L. Coles, G. Williams, A. Rutman, P.M. Goggin, E.C. Adam, A. Page, H.J. Evans, P.M. Lackie, C. O'Callaghan, J.S. Lucas, *PLoS One* **2014**, 9, e89675.
- [41] R.A. Hirst, A. Rutman, G. Williams, C. O'Callaghan, *Chest* **2010**, 138, 1441.
- [42] D.D.H. Lee, A. Petris, R.E. Hynds, C. O'Callaghan, *Methods Mol. Biol.* **2020**, 2109, 275.
- [43] C. Smith, H. Kulkarni, P. Radhakrishnan, A. Rutman, M. Bankart, G. Williams, R. Hirst, A. Easton, P. Andrew, C. O'Callaghan, *Eur. Resp. J.* **2014**, 43, 485.
- [44] M. Chilvers, A. Rutman, C. O'Callaghan, *J. Allergy Clin. Immunol.* **2003**, 112, 518.
- [45] M.A. Chilvers, A. Rutman, C. O'Callaghan, *Thorax* **2003**, 58, 333.
- [46] C.M. Rossman, R.M. Lee, J.B. Forrest, M.T. Newhouse, *Am. Rev. Respir. Dis.* **1984**, 129, 161.
- [47] C. Frantz, K. Stewart, V. Weaver, *J. Cell Sci.* **2010**, 123, 4195.
- [48] J. Schagen, P. Sly, E. Fantino, *Lab. Invest.* **2018**, 98, 1478.
- [49] E. Bayart, O. Cohen-Haguener, *Curr. Gene Ther.* **2013**, 13, 12.
- [50] N. Mehrban, C. Pineda Molina, L. Quijano, J. Bowen, S. Johnson, J. Bartolacci, J. Chang, S. DA, D. Woolfson, M. Birchall, S. Badylak, *Acta Biomater.* **2020**, 111, 141.
- [51] N. Recek, M. Jaganjac, M. Kolar, L. Milkovic, M. Mozetic, K. Stana-Kleinschek, A. Vesel, *Molecules* **2013**, 18, 12441.
- [52] G. Anand, S. Sharma, A. Dutta, S. Kumar, C. Balford, *Langmuir* **2010**, 26, 10803.
- [53] M. Rankle, T. Ruckstuhl, M. Rabe, G. Artus, A. Walser, S. Seeger, *ChemPhysChem* **2006**, 7, 837.
- [54] M. Rabe, D. Verdes, S. Seeger, *Adv. Colloid Interface Sci.* **2011**, 162, 87.
- [55] W. Norde, C. Giacomelli, *J. Biotechnol.* **2000**, 79, 259.
- [56] J. Škvarla, *Adv. Colloid Interface Sci.* **2001**, 91, 335.
- [57] A. Minton, *Biophys. J.* **2001**, 80, 1011.
- [58] M. Rabe, D. Verdes, S. Seeger, *Soft Matter* **2009**, 5, 1039.
- [59] T. Weidner, N. Samuel, K. McCrea, L. Gamble, R. Ward, D. Castner, *Biointerphases* **2010**, 5, 9.

Author Contributions

NM, DC, JB and MAB designed the project. DAS manufactured the peptides and NM and SCG plasma treated the samples. NM and JB conducted the material characterisation studies while NM, DDHL and DC carried out the cell culture experiments. HD, DNW, MAB and CO supervised the work and raised grant support. NM, JB and DC wrote the paper.

Conflict of Interest

The authors do not have a financial/commercial Conflict of Interest.

CRedit author statement

NM, DC, JB and MAB: Conceptualization. **NM, DC, JB and SCG:** Methodology, Validation, Formal analysis, Investigation. **DAS, DDHL:** Investigation. **HD, DNW, MAB and CO:** Resources, Funding acquisition, Supervision. **NM, JB, DC:** Visualization, Writing-Original Draft, Writing-Review & Editing.

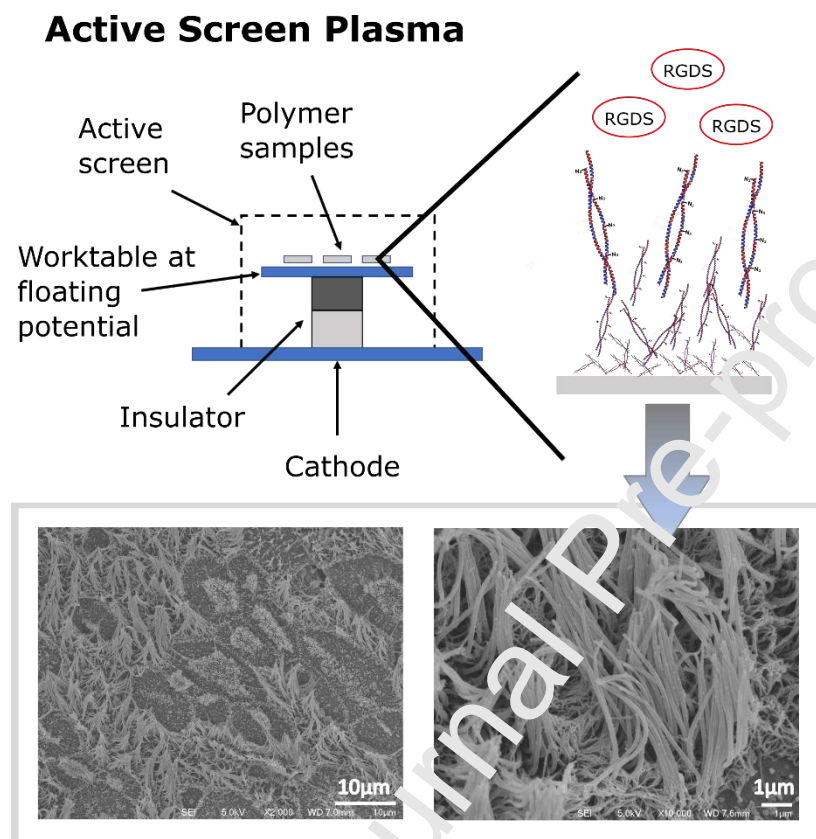
Declaration of interests

The authors declare that they have no known competing financial interests or personal relationships that could have appeared to influence the work reported in this paper.

The authors declare the following financial interests/personal relationships which may be considered as potential competing interests:

Journal Pre-proof

Graphical Abstract



Active screen plasma treatment enables the adsorption of α -helical peptides onto polymers. These chemically and physically controllable peptides promote the differentiation of human nasal epithelial cells. Tight junctions and cilia which beat spontaneously at a normal expected frequency are observed after 28 days. This study presents strategies in improving cellular response to implantable polymers towards aerodigestive tract reconstruction and regeneration.

HIGHLIGHTS

- α -Helical peptides can promote functional differentiation of cells on polymers
- Plasma treatment promotes α -helical peptide adsorption to polymers
- Adsorbed peptides support human nasal epithelial cell differentiation at an air-liquid interface
- Differentiated epithelial cells form tight junctions and produce beating cilia after 28 days

Journal Pre-proof